MATHEMATICAL ANALYSIS AND OPTIMIZATION OF DESIGN CHARACTERISTICS OF STABILIZING VERTEBRAL BODY REPLACING SYSTEMS FOR SUBAXIAL CERVICAL FUSION USING THE FINITE ELEMENT METHOD

A.S. Nekhlopochin[1, 2], S.N. Nekhlopochin[1, 2], M.Y. Karpinsky[3], A.I. Shvets[2], E.D. Karpinskaya[3], A.V. Yaresko[3]
[1]Lugansk Regional Clinical Hospital, Lugansk, Ukraine
[2]Lugansk State Medical University, Lugansk, Ukraine;
[3]Sytenko Institute of Spine and Joint Pathology, Kharkov, Ukraine

Objective. To analyze the characteristics of the stress-strain state of the cervical spine when replacing vertebral body with implants of different design.
Material and Methods. Mathematical modeling was performed by developing three finite element models of the cervical spine. The models simulated human cervical spine within C3—C7 spinal segment. The C5 vertebra was replaced by three different systems: mesh cage, mesh cage combined with anterior plate, and telescopic vertebral body replacement implant fixed to the bodies. The stress-strain state of models was studied under four variants of loading: compression, flexion, extension, and rotary impact.
Results. Stress intensity values were obtained for the following structures: top of the vertebral body, bottom of the vertebral body, pedicle, lamina, joint masses, teeth and screws (if any) of instrumentation under different loading options.
Conclusion. The presence of an additional fixation to vertebral bodies allows reducing the level of maximum stress in the bone tissue of vertebrae contacting the implant. Telescopic cage shows the lowest level of stress in the model elements under compression and flexion. Stress indicators in extension and rotation have minor differences between different sites.
Key Words: anterior fusion, finite element model, telescopic implant for vertebral boby replacement.

Please cite this paper as: *Nekhlopochin AS, Nekhlopochin SN, Karpinsky MY, Shvets AI, Karpinskaya ED, Yaresko AV. Mathematical analysis and optimization of design characteristics of stabilizing vertebral body replacing systems for subaxial cervical fusion using the finite element method. Hir. Pozvonoc. 2017;14(1):37—45. In Russian. DOI: http://dx.doi.org/10.14531/ss2017.1.37-45.*

At the present time, practicing traumatologists and orthopedists have at their disposal various vertebral body replacement systems that enable decompressive-stabilizing and reconstructive surgery of the spine from the ventral approach [4].

Biomechanical and pathomorphological techniques that are essential when solving disputable issues arising both in research and clinical practice of spinal surgery, in particular, cervical spine surgery, are used to select the optimal devices and methods for their fixation and fusion methods themselves [14, 19].

The wide range of these research includes experimental biomechanical studies of the anatomical specimens of the human cervical spine [8, 12], anatomical specimens of the cervical spine of laboratory animals, including implantation of prosthetic vertebral bodies and discs [13, 21].

These methods are often replaced by advanced technique, which does not require experiments on animals or anatomical preparations, such as mathematical modeling, finite element method (FEM) being one of its variants [6, 7, 11, 18, 24]. Experimental studies of the biomechanical characteristics of the spine using the FEM have been carried out as early as in 1973 [23, 25].

Later on, FEM was started to be used for the mathematical modeling of human cervical spine. [24] In 1996, Yoganandan et al. [23] reported the development of the mathematical model of the C4–C6 on the basis of CT slices in increments of 1 mm and cryomicrotomy.

Mathematical modeling with FEM is used not only to study the biomechanical properties of spine segments, but also to measure biomechanical characteristics of the anterior interbody fusion with various implants [9, 10, 15–17, 20, 22].

The research was aimed at analyzing the characteristics of the stress-strain state of the cervical spine after vertebral body replacement with artificial implants of various designs.

Material and Methods

Mathematical modeling using FEM was carried out at the laboratory of biomechanics of the Institute of Spine and Joint Pathology n.a. prof. M.I. Sytenko. Three finite element models of the cervical spine were built in order to solve this problem (Fig. 1).

The models simulated the C3–C7 segment of the human cervical spine,

including the intervertebral discs and facet joints with the interarticular cartilage. Bonded-type contact was used between the vertebral bodies and intervertebral discs, as well as in the facet joints. The C5 vertebra was replaced by three different constructs: mesh cage (Fig. 1a), mesh cage with additional fixation of the adjacent vertebra with a plate (Fig. 1b), and cage with original design fixation elements, telescopic vertebral body replacement implants (TVBRI; Fig. 1c) [5].

Additionally, TVBRI model was used to simulate the functioning of the cage with large and small teeth (Fig. 2).

The implant model with large teeth had 4 teeth on each of the upper and lower planes, whose length exceeded the thickness of the cortical layer of the vertebra. The implant model with small teeth had 10 teeth on each of the upper and lower planes, the length of the teeth corresponded to the half-thickness of the cortical layer of the vertebra.

Mechanical properties of biological tissues were used in the simulation [2]. Mechanical properties of the materials are shown in the Table.

The stress-strain state of the models was studied with four loading options: compression, extension, flexion, and rotary impact. Loading schemes of the models are shown in Fig. 3.

The models had rigid fixation at the lower plane of C7 vertebral body and its facet joints (Fig. 3a). The load value on the model was 100 N. Compression load was provided by distributed load of 36 N on the upper surface of C3 vertebral body and 32 N on the upper plane of its facet joints (Fig. 3b). Flexion was simulated by 100 N load on the anterior edge of C3 vertebral body (Fig. 3c), and extension was simulated by 50 N load on its arches (Fig. 3d). Rotation load was provided by applying 100 N force on the upper surface of C3 vertebral body (Fig. 3e).

The model consists of 145 282 tetrahedral 10-node isoparametric finite elements and has 245,105 nodes. The von Mises criterion was selected to assess stress-deformed state of the models [3].

The models were built using the SolidWorks software package, FEM calculations were carried out using COSMOSWorks software implemented in this package [1].

Results and Discussion

The study provided the picture of the stress-strain state of the cervical spine models, where the body of the C5 vertebra was replaced by three types of implants.

Fig. 4 shows stress distribution pattern in the models under axial compression load.

In all models, most of the load was accommodated by metal structures, however, some features are observed in the bone tissue.

During compression load in the bone tissue of the vertebral bodies, main differences were observed in C4 and C6 vertebrae adjacent to the damaged one. The highest stress values were observed in the cage model without additional fixation. Thus, maximum stress values on the upper surface of C4 and C6 vertebral bodies are 3.0 and 10.0 MPa, respectively. In the models with additional fixation, stress level in these areas is significantly lower. While stress values on the upper surface of C4 vertebra in the models with plate and TVBRI are virtually identical, amounting to 2.6 and 2.7 MPa, respectively, the differences are more significant in C6 vertebra, being 7.2 and 5.8 MPa. On the bottom surface of C4 and C6 vertebrae, stress distribution pattern is almost identical. The greatest differences are observed on the surface of the vertebra contacting with the cage, that is, the bottom surface of C4 vertebra, being 7.9, 6.1, and 5.5 MPa, respectively, for the models with a cage, anterior plate, and TVBRI. The pedicles of C6 vertebral arches were the most loaded part of the vertebrae. In this area, maximum stress value was 18.2 MPa for the model without additional fixation, 17.2 MPa for the model with the anterior plate, and 16.5 MPa for the model with TVBRI. In the pedicles of the arches of other vertebrae, stress level was much lower with minor differences. The greatest differences in the stress values in the facet joints are observed in C4 and C5 vertebrae. In these areas, the cage model without additional fixation demonstrated the worst performance, 2.9 MPa in C4 vertebra and 1.9 MPa in C5 vertebra. Application of TVBRI results in more effective unloading of the facet joints, 2.6 MPa for C4 vertebra and 1.5 MPa for C5 vertebra. The model with anterior plate showed intermediate values, 2.8 and 1.6 MPa in the respective zones. The lowest stress on the cage teeth occurs in the models with TVBTI, 2.9 and 2.1 MPa for C4 and C6 vertebrae, respectively. In the structure with plate, these values are

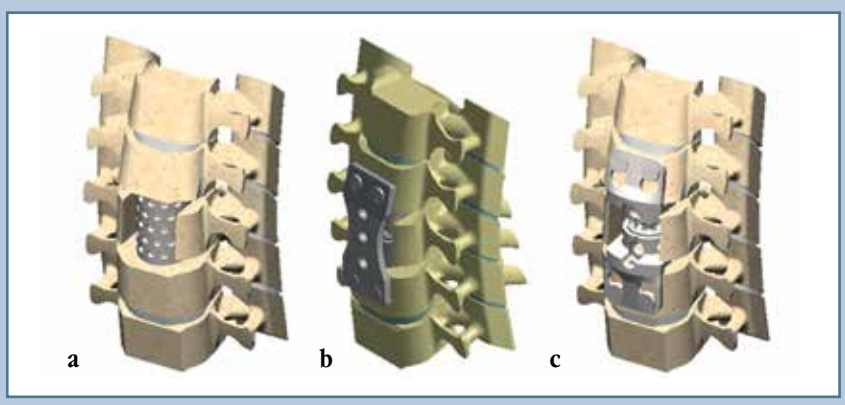

Fig. 1
The models of the cervical spine with implants: **a** – mesh cage; **b** – cage with the anterior plate; **c** – telescopic vertebral body replacement implant

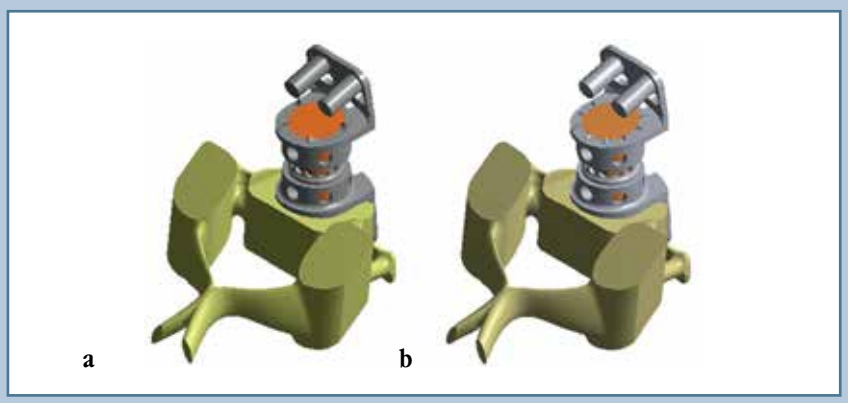

Fig. 2
Cervical spine models with telescopic vertebral body replacement implant: **a** – with large teeth; **b** – with small teeth

Table
Mechanical properties of the materials used in the simulation

Material	Young's elasticity modulus, MPa	Poisson's ratio	Tensile strength, MPa
Cortical bone	100 00.0	0.30	145
Spongy bone	450.0	0.20	10
Articular cartilage	10.5	0.49	–
Intervertebral disc	4.2	0.45	–
Porous ceramic	67 000.0	0.30	–
Titanium BT-16	110 000.0	0.30	235

twice higher, 5.9 and 4.2 MPa. Stress values on TVBRI teeth are 5.5 and 3.5 MPa for C4 and C6 vertebrae, respectively, which is significantly lower than in the model with plate (8.9 and 9.8 MPa) and in the model without additional fixation (10.2 and 12.5 MPa).

Investigations of the models under compression load showed that the use of additional fixation reduces the stress level in the bone tissue of the vertebrae, when substituting vertebral body with cage. TVBRI is more effective from this viewpoint.

The next stage includes the modeling of the functioning of the corresponding implants in neck extension position. Stress distribution pattern associated with this load in the test models is shown in Fig. 5.

The major load is accommodated by the metal structures, similarly to the results of the previous study.

Let us analyze the absolute values of the maximum stresses arising in the bone structures of the models.

The greatest stresses in the vertebral bodies occur at the points of their contact with cages, similarly to the study with compression, i.e. the lower surface C4 vertebra and the upper surface of C6 vertebral body. In the first case, stress value is 9.0, 8.1, and 5.0 MPa for the models without additional fixation, with the anterior plate,

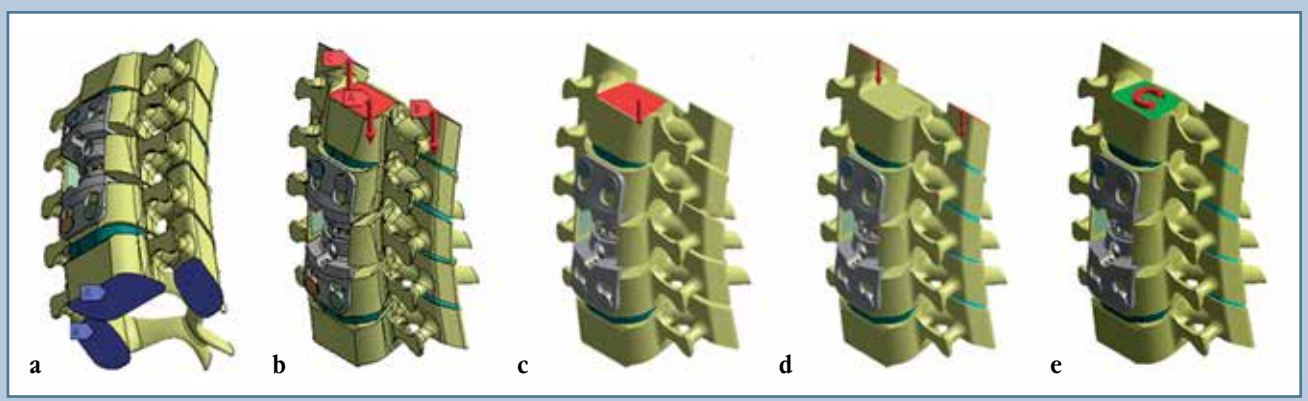

Fig. 3
Model loading schemes: **a** – fixation of the models at the lower surface of C7 vertebra; **b** – compression loading; **c** – flexion loading; **d** – extension loading; **e** – rotational loading

and TVBRI, respectively. In the second case, stress level is 10.3, 6.5, and 4.1 MPa for the respective models. In the neck flexion position, the pedicles of the vertebral arches are unloaded and stress value does not exceed 1.5 MPa in the arches of C6 vertebra in the model without additional fixation. In two other models, stress values in this area are 1.1 MPa. In this case, facet joints are virtually unloaded, stress level does not reach the level of 1.0 MPa without any significant differences between the models. Major changes in stress distribution are observed in the fixation elements of the structure. The greatest load falls on the upper fixation elements located on the body of C4 vertebra. Thus, the stress level on the fixation screws in this area is 15.8 MPa for the model with the anterior plate and 12.3 MPa for TVBRI. The maximum stress values on the screws in the vertebral body C6 are somewhat lower and amounts to 11.8 and 6.1 MPa for the models with extramedullary plate and our structure, respectively. As for the teeth on the cage contact plane, the maximum stresses arise on the teeth of the cage without additional fixation and amount to 20.9 MPa on the side of C4 vertebra and 27.0 MPa on the side of C6 vertebra. This is twice higher than the maximum stress value when using TVBRI, being 13.0 and 10.2 MPa, respectively. The structure with the anterior plate demonstrated the smallest stress values in these areas, 9.9 and 7.2 MPa, respectively.

Thus, contact points between the vertebral bodies and cage teeth are the most loaded area in the neck flexion position, the lowest stress level in this area demonstrated the model with the anterior plate. The lowest stress level in the other areas was observed in a model with TVBRI.

The stress-strain state pattern in the models in neck extension position is shown in Fig. 6.

It can be seen that the main load is still accommodated by metal structures. In the bony structures, stress shifts to the posterior column.

In the neck extension position, peak stress points correspond to vertebra-cage contact points, similarly to the results of previous studies. Maximum stress value on the upper surface of C6 vertebra is 3.8 MPa for the model without additional fixation, 2.6 MPa for the model with the anterior plate, and 2.9 MPa for the TVBRI. Maximum stress level on the bottom surface of C4 vertebral body reaches the value of 11.6, 7.6, and 7.5 MPa for the respective models. Since the main load is shifted to the posterior column, maximum stress values are observed in the pedicles of C6 vertebral arches: 20.7 MPa for the model without additional fixation, 20.2 MPa for the model with the anterior plate, and 22.4 MPa for the TVBRI. In C4 vertebral arches, where stress level is the lowest in the cage model without additional fixation, amounting to 7.5 MPa, additional fixation leads to increased stress in C4 vertebral arches in neck extension position, being 10.0 MPa in the case of fixation with the plate and 9.6 MPa in the case of the TVBRI. Stress also increases in the facet joints. Maximum stress values occur in C4 and C6 vertebrae. Additional fixation has a positive effect on stress distribution in those areas. While the cage without fixation increases stress up to 3.9 MPa in the joints of C4 vertebra and up to 4.1 MPa in the joints of C6 vertebra, in the models with additional fixation, stress level in C4 vertebral joint is 3.8 MPa and 3.7 in the models with the plate and TVBRI, respectively, and stress level in C6 vertebral joints is 3.5 MPa in both models. The screws in C4 vertebral body remain the most highly loaded elements, just as in the case of neck flexion, amounting to 10.2 MPa for the model with the plate and 7.6 MPa for the TVBRI. Our cage structure also results in more sparing loading of the screws in C6 vertebra (4.4 MPa) compared to the extramedullary plate (7.6 MPa). As for the teeth, the structure with the plate is superior to the other options, 9.8 MPa on C4 vertebra and 11.1 MPa on C6 vertebra. TVBRI and the cage without additional support lead to increase in teeth stress on the side of C4 vertebra to 12.9 and 12.5 MPa, respectively, and to 14.5 and 17.8 MPa on the side of C6 vertebral body.

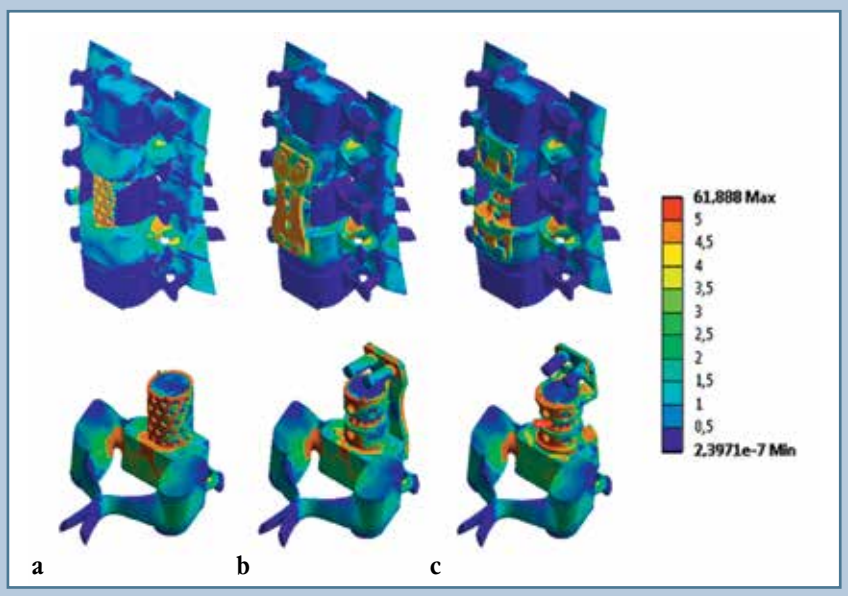

Fig. 4
Stress distribution in the models under the compression load: **a** – mesh cage (front and rear view); **b** – mesh cage with the anterior plate (front and rear view); **c** – telescopic vertebral body replacement implant (front and rear view)

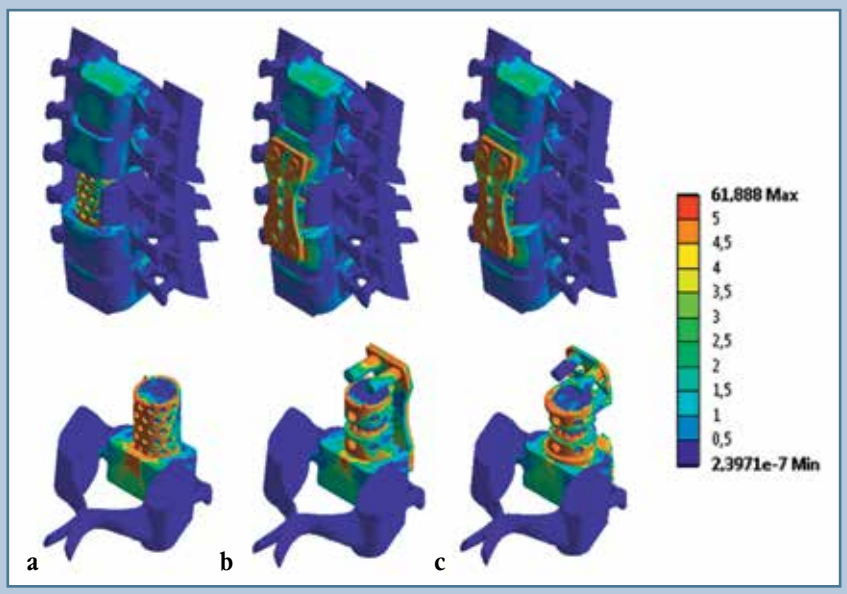

Fig. 5
Stress distribution in the models in the neck flexion position: **a** – mesh cage (front and rear view) **b** – mesh cage with extramedullary plate (front and rear view); **c** – telescopic vertebral body replacement implant (front and rear view)

It is difficult decide between tested structures when analyzing stress distribution in the models in neck extension position, since this load leads to an ambiguous stress distribution. We can conclude that the behavior of the models with various structures is virtually equivalent in the neck extension position.

Fig. 7 shows the pictures of the stress-strain state models under rotational load.

In this case, the structures unload the damaged C5 vertebra, but lead to excessive stress in adjacent vertebrae.

The maximum rotation-induced stress occurs in the elements of C3 vertebra, the first flexible element in the "spine–implant" system, and reaches 4.9 MPa in the model without additional fixation and 4.8 MPa in the models with additional fixation of the implant. Conventionally high stress levels are observed in the bodies of C4 and C6 vertebrae. Thus, stress values are up to 3.7 MPa on the lower surface of C4 vertebra for the model without additional fixation and 3.3 and 2.0 MPa in the models with additional fixation of the implant with plate and TVBRI, respectively. Stress values on the upper surface of C6 vertebral body reach 4.0, 2.9, and 2.7 MPa for the respective models. In the pedicles of the vertebral arches, the highest stress level was detected in C3 and C6 vertebrae in the model without additional cage fixation, being 13.8 and 10.3 MPa, respectively. In the models with additional cage fixation, stress leveles in the pedicles of C3 and C6 vertebral arches are lower, 10.5 and 6.0 MPa, respectively, for the model with extramedullary plate, 11.5 and 5.2 MPa for the model with the TVBRI. In the case of rotation, high stress level is also observed in the laminas of the vertebral arches and reaches maximum values in C6 vertebra, 6.5 MPa in the model without additional fixation and 5.8 and 5.7 MPa in the models with additional implant fixation with the plate and TVBRI, respectively. In the facet joints, stress intensity in C3 and C6 vertebrae decreases to the level of 2.0–2.2 MPa without significant differences between the models. As for fixation elements of the implant, there is notably very low stress level on the screws of the TVBRI, 3.2 MPa in C4 vertebra and 0.6 MPa in C6, while in the model with the anterior plate these parameters reach the level of 8.9 and 5.7 MPa, respectively. The opposite situation is observed on the cage teeth. The lowest stress level was recorded in the model with the plate, 4.8 and 5.4 MPa on the sides of C4 and S6 vertebrae, respectively.

In the model with the TVBRI, these values are 4.3 and 9.8 MPa. In the model without additional fixation, they are 6.5 and 14.3 MPa, respectively.

Investigation of the stress-deformed state of the models under rotational load showed that additional fixation leads to redistribution of stress intensity from the cage teeth to additional fixation elements.

The next stage of the study included investigation of the impact of cage teeth size on the stress distribution pattern in the "cervical spine–implant" system. The experience of previous studies has shown that the main peak stress area occurs at the contact points between the implant and bone fragments. Therefore, C4 and C6 vertebrae were selected to analyze stress-strain state. Fig. 8 shows stress distribution patterns in C6 vertebrae of the models with all load types.

The vertebrae in the model with large teeth are less intensely colored, which is indicative of lower stress level. Stress value is very low inside the teeth (less than 0.5 MPa). In the model with small teeth, elevated stress zones are larger and arranged over the whole vertebral body surface.

Conclusions

1. The presence of additional fixation reduces the maximum stress level in the bone tissue of the vertebrae contacting with the implant.

2. In our structure, cage showed the lowest stress level in the elements of the model under compression loads and neck flexion. In the case of neck extension and rotation, stress values at different sites have minor differences in one or another direction in both models.

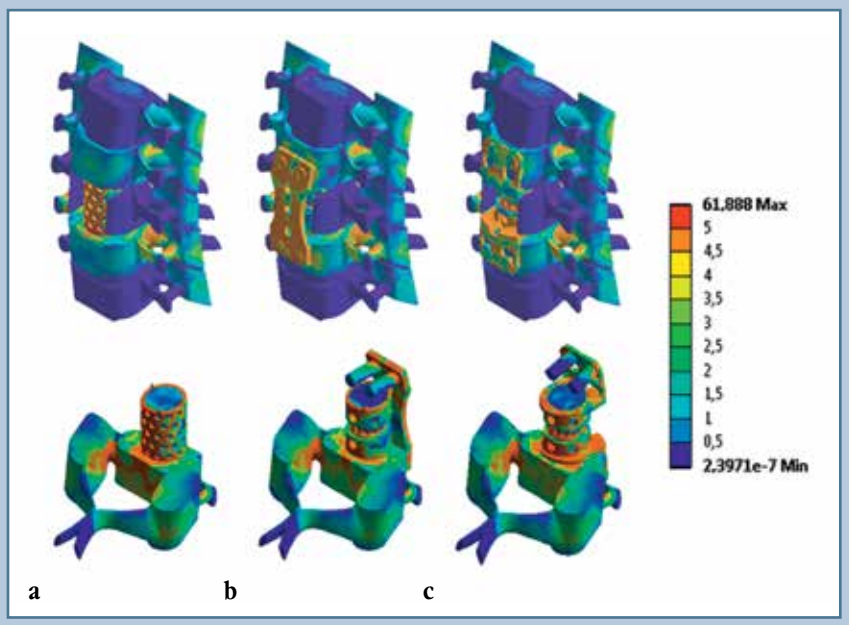

Fig. 6
Stress distribution in the models in the neck extension position: **a** – mesh cage (front and rear view) **b** – mesh cage with extramedullary plate (front and rear view); **c** – telescopic vertebral body replacement implant (front and rear view)

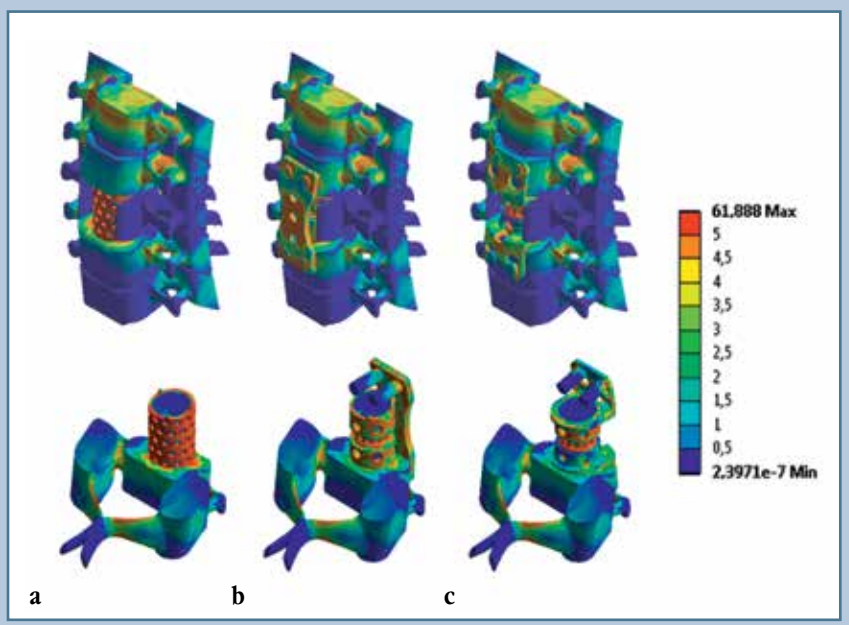

Fig. 7
Stress distribution in the models during rotation movements: **a** – mesh cage (front and rear view) **b** – mesh cage with the anterior plate (front and rear view); **c** – telescopic vertebral body replacement implant (front and rear view)

3. The use of four large teeth perforating the cortical bone of the vertebral body results in lower stress values in the contacting vertebral bone structures compared to the structure having larger number of shorter teeth.

The study was not sponsored. The authors declare no conflict of interest.

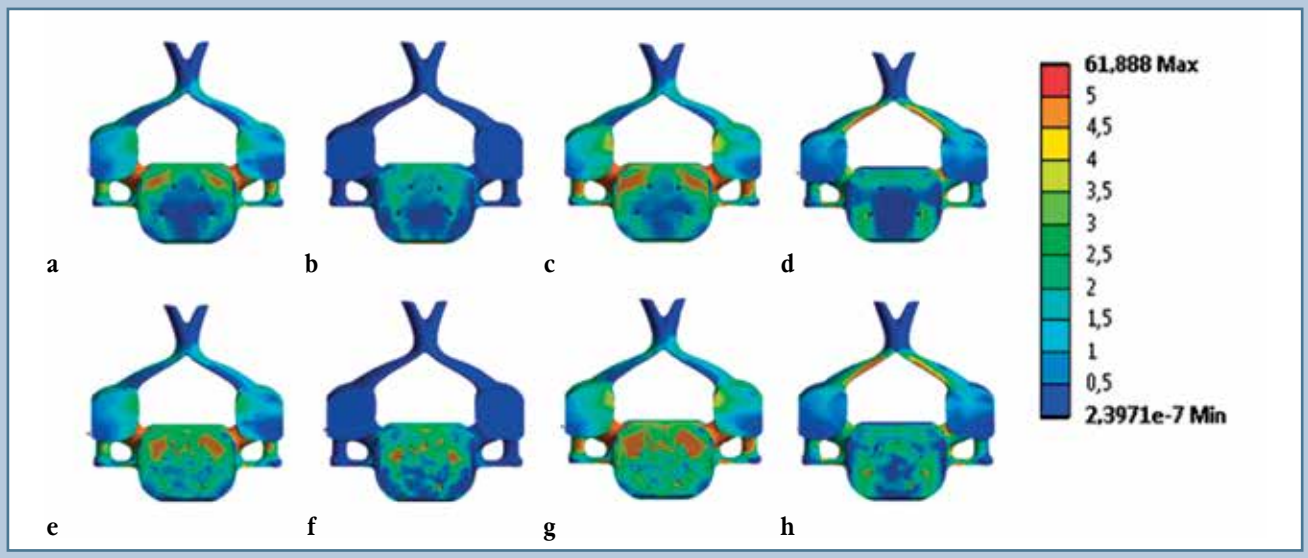

Fig. 8
Stress distribution in the body of C6 vertebra in the models with different teeth sizes for all loading types: **a** – large teeth, compression load, **b** – large teeth, neck flexion; **c** – large teeth, neck extension; **d** – large teeth, torsional load; **e** – small teeth, compression load; **f** – small teeth, neck flexion; **g** – small teeth, neck extension; **h** – small teeth, torsional load

References

1. **Alyamovsky AA.** SolidWorks/COSMOSWorks. Engineering Finite Element Analysis. Moscow: Designing, 2004. 432 p. In Russian.
2. **Berezovsky VA, Kolotilov NN.** Biophysical Characteristics of Human Tissue: Handbook. Kiev, 1990. In Russian.
3. **Zenkevich O.** Finite Element Method in Technics. Moscow: Mir, 1975. In Russian.
4. **Nekhlopochin AS.** Vertebral body replacement systems for anterior fusion: literature review. Hir Pozvonoc. 2015;12(2):20–24. In Russian. DOI:10.14531/ss2015.2.20-24.
5. **Nekhlopochin AS, Shvets AI, Nekhlopochin SN.** A telescopic vertebral endoprosthesis for subaxial cervical fusion. Voprosy nejrokhirurgii imeni N.N. Burdenko. 2016;80(1):19–26. In Russian. DOI:10.17116/neiro201680119-26.
6. **Radchenko VA, Shimon VM, Tkachuk NA, Shman'ko AP.** Finite element models to assess the stiffness and strength of ceramic hydroxylapatite implants. Orthopaedics, Traumatology and Prosthetics. 2002;(3):60–64. In Russian.
7. **Filipenko VA, Miteleva ZM, Ziman ZZ, Mezentsev VO, Yaresko OV.** Finite element method in clinical biomechanics and forecasting results of bone cavity plasty with calcium-phosphate ceramics. Orthopaedics, Traumatology and Prosthetics. 2006;(2):34–41. In Ukrainian.
8. **Bozkus H, Ames CP, Chamberlain RH, Nottmeier EW, Sonntag VK, Papadopoulos SM, Crawford NR.** Biomechanical analysis of rigid stabilization techniques for three-column injury in the lower cervical spine. Spine. 2005;30:915–922. DOI: 10.1097/01.brs.0000158949.37281.d7.
9. **Gilbertson LG, Goel VK, Kong WZ, Clausen JD.** Finite element methods in spine biomechanics research. Crit Rev Biomed Eng. 1995;23:411–473. DOI: 10.1615/CritRevBiomedEng.v23.i5-6.20.
10. **Goel VK, Gilbertson LG.** Applications of the finite element method to thoracolumbar spinal research – past, present, and future. Spine. 1995;20:1719–1727.
11. **Graham RS, Oberlander EK, Stewart JE, Griffiths DJ.** Validation and use of a finite element model of C-2 for determination of stress and fracture patterns of anterior odontoid loads. J Neurosurg. 2000;93(1 Suppl):117–125.
12. **Hart R, Gillard J, Prem S, Shea M, Kitchel S.** Comparison of stiffness and failure load of two cervical spine fixation techniques in an in vitro human model. J Spinal Disord Tech. 2005;18 Suppl:S115–S118. DOI: 10.1097/01.bsd.0000132288.65702.6e.
13. **Kandziora F, Pflugmacher R, Schefer J, Born C, Duda G, Haas NP, Mittlmeier T.** Biomechanical comparison of cervical spine interbody fusion cages. Spine. 2001;26:1850–1857. DOI: 10.1097/00007632-200109010-00007.
14. **Kim SB, Bak KH, Cheong JH, Kim JM, Kim CH, Oh SH.** Biomechanical testing of anterior cervical spine implants: evaluation of changes in strength characteristics and metal fatigue resulting from minimal bending and cyclic loading. J Korean Neurosurg Soc. 2005;37:217–222.
15. **Kumaresan S, Yoganandan N, Pintar FA.** Finite element analysis of anterior cervical spine interbody fusion. Biomed Mater Eng. 1997;7:221–230.
16. **Maiman DJ, Kumaresan S, Yoganandan N, Pintar FA.** Biomechanical effect of anterior cervical spine fusion on adjacent segments. Biomed Mater Eng. 1999;9:27–38.
17. **Natarajan RN, Chen BH, An HS, Andersson GB.** Anterior cervical fusion: a finite element model study on motion segment stability including the effect of osteoporosis. Spine. 2000;25:955–961.
18. **Ng HW, Teo EC.** Nonlinear finite-element analysis of the lower cervical spine (C4-C6) under axial loading. J Spinal Disord. 2001;14:201–210. DOI: 10.1097/00002517-200106000-00003.

19. **Panjabi MM.** Cervical Spine Models for Biomechanical Research. Spine. 1998;23:2699–2700. DOI: 10.1097/00007632-199812150-00008.
20. **Pitzen TR, Matthis D, Barbier DD, Steudel WI.** Initial stability of cervical spine fixation: predictive value of a finite element model. Technical note. J Neurosurg. 2002;97(1 Suppl):128–134. DOI: 10.3171/spi.2002.97.1.0128.
21. **Rapoff AJ, O'Brien TJ, Ghanayem AJ, Heisey DM, Zdeblick TA.** Anterior cervical graft and plate load sharing. J Spinal Disord. 1999;12:45–49. DOI: 10.1097/00002517-199902000-00007.
22. **Teo EC, Yang K, Fuss FK, Lee KK, Qiu TX, Ng HW.** Effects of cervical cages on load distribution of cancellous core: a finite element analysis. J Spinal Disord Tech. 2004;17:226–231. DOI: 10.1097/00024720-200406000-00010.
23. **Yoganandan N, Kumaresan SC, Voo L, Pintar FA, Larson SJ.** Finite element modeling of the C4-C6 cervical spine unit. Med Eng Phys. 1996;18:569–574. DOI: 10.1016/1350-4533(96)00013-6.
24. **Yoganandan N, Kumaresan S, Voo L, Pintar FA.** Finite element applications in human cervical spine modeling. Spine. 1996;21:1824–1834.
25. **Yoganandan N, Myklebust JB, Ray G, Sances A Jr.** Mathematical and finite element analysis of spine injuries. Crit Rev Biomed Eng. 1987;15:29–93.

Address correspondence to:
Nekhlopochin Aleksey Sergeyevich
Kurchatova str., 9–34,
Lugansk, 91031, Ukraine,
AlexeyNS@gmail.com

Received 19.09.2016
Review completed 03.10.2016
Passed for printing 06.10.2016

Aleksey Sergeyevich Nekhlopochin, teaching assistant of the Department of Neurology and Neurosurgery, Lugansk State Medical University, Head of the Department of Neurosurgery, Lugansk Regional Clinical Hospital, Lugansk, Ukraine, AlexeyNS@gmail.com;
Sergey Nikolayevich Nekhlopochin, MD, PhD, teaching assistant of the Department of Neurology and Neurosurgery, Lugansk State Medical University, resident in the Department of Neurosurgery, Lugansk Regional Clinical Hospital, Lugansk, Ukraine, nsna56@mail.ru;
Mikhail Yuryevich Karpinsky, researcher, Biomechanics Laboratory, Sytenko Institute of Spine and joint Pathology, Kharkov, Ukraine, korab.karpinsky9@gmail.com;
Aleksey Ivanovich Shvets, MD, DMSc, Prof. of the Department of Hospital Surgery, Traumatology and Orthopaedics, Lugansk State Medical University, Lugansk, Ukraine, shvalex42@gmail.com;
Elena Dmitryevna Karpinskaya, junior researcher, Biomechanics Laboratory, Sytenko Institute of Spine and Joint Pathology, Kharkov, Ukraine, helen.karpinska@gmail.com;
Alexandr Vasilyevich Yaresko, junior researcher, Biomechanics Laboratory, Sytenko Institute of Spine and joint Pathology, Kharkov, Ukraine, avyresko@gmail.com.